

RESEARCH

Open Access



Muscle-to-action mapping for intuitive training of muscle synergies in post-stroke upper-limb rehabilitation

Hangil Lee^{1†}, Jeong-Ho Park^{1†}, Joon-Ho Shin², Jinsook Roh³ and Hyung-Soon Park^{1*}

Abstract

Background Effective motor task execution relies on precise muscle coordination, which is often disrupted after a stroke, leading to impaired motor functions. Post-stroke, alterations in intermuscular coordination, including abnormal coupling of shoulder abductor muscles, are commonly observed and contribute to these impairments. Traditional rehabilitation often overlooks this complex intermuscular coordination, and there is a need for intuitive strategies to modify abnormal muscle synergies.

Objective This study introduced a novel “muscle-to-action mapping” approach to alter activation profiles of stroke affected muscle synergies. Muscle-to-action mapping trains complex muscle synergies by mapping them to intuitive motions or force directions. By mimicking target actions, patients can achieve desired muscle activation patterns. The feasibility of this approach for correcting abnormal intermuscular coordination and improving force control during reaching was tested in stroke survivors.

Methods A force tracking training system using muscle-to-action mapping was developed to modify abnormal synergy activation profiles during isokinetic reaching tasks. The system guided muscle activation by predicting the direction of endpoint force needed to activate specific muscle synergies, deviating from habitual patterns. The system’s effectiveness was evaluated in eleven chronic stroke survivors, measuring changes in muscle synergies, endpoint force control, and clinical assessment scores.

Results The intervention significantly enhanced targeted muscle synergy activations and endpoint force control, demonstrating the training’s ability to induce desired muscle synergy activation profiles through muscle-to-action mapping. The overall structure of muscle synergies remained mostly unchanged post-training, highlighting the potential to modify activation profiles without altering synergy vectors. Functional improvements were reflected in the Fugl-Meyer Assessment for the Upper Extremity and Wolf Motor Function Test scores, which increased by 3.36 and 6.45 points, respectively.

Conclusion This study validates muscle-to-action mapping for training muscle synergy activation profiles in stroke survivors. Using a biomechanical model to generate endpoint forces, this method effectively altered synergy activation profiles and improved force control during reaching tasks, leading to clinical improvements. These findings indicate that muscle-to-action mapping could be a valuable addition to stroke rehabilitation, offering an intuitive method for enhancing intermuscular coordination and motor recovery.

[†]Hangil Lee and Jeong-Ho Park have contributed equally to this work.

*Correspondence:
Hyung-Soon Park
hyungspark@kaist.ac.kr
Full list of author information is available at the end of the article



Trial registration: Registered in Clinical Research Information System of Korea National Institute of Health (KCT0005803).

Keywords Intermuscular coordination, Muscle synergy, Muscle-to-action mapping, Stroke, Upper limb, Neurorehabilitation, Force control

Background

The successful execution of motor tasks is fundamentally reliant on the precise coordination of muscle activations [1–3]. The analysis of intermuscular coordination has been grounded in the concept of muscle synergies, the balance of multiple muscles activations frequently co-activated as a motor module during specific motor tasks. Muscle synergies consist of synergy vectors, which represent specific patterns of muscle activation weights, and their associated activation profiles, which are the time-varying coefficients that represent when and to what extent these synergy vectors are activated to produce coordinated movements. Previous studies have suggested that the formation of these muscle synergies stems from various neuroanatomical structures and mechanisms, such as interneuron networks within the central nervous system that transmit motor commands to multiple muscles, and the distributed representations of muscles within the motor cortex [4–6]. Such neural underpinnings suggest that any reorganization of the brain, whether due to motor learning or neurological injury, could influence both the structure and activation profile of muscle synergy vectors.

In the context of sports, training among elite athletes showcases positive neural adaptations, where muscle synergies are fine-tuned for enhanced performance [7–9]. Differences in synergy vectors and activation profiles observed between elite and amateur athletes illustrate the capability of targeted training to reinforce neural pathways, leading to optimized kinematic outputs. For example, certain muscle synergies exclusive to elite runners were associated with improved running efficiency, while elite and amateur swimmers and archers exhibited comparable synergy vectors, differing primarily in activation timing [9–11].

Conversely, in the field of neurorehabilitation, changes in muscle synergies following a stroke are associated with compromised motor functions in affected limbs [12–14]. These impairments manifest as alterations in synergy number, vector composition, and activation profiles [14–19], reflecting the interdependent nature of these components. Our previous study demonstrated that while stroke survivors exhibited one fewer synergy than neurologically intact individuals (stroke: 4 vs control: 5) under constrained isokinetic reaching conditions, standardizing synergy extraction to five revealed comparable synergy vectors between groups [20]. However,

stroke participants still displayed distinct abnormalities in synergy activation that were linked to unintended force coupling during reaching tasks [21]. Similarly, other studies have shown that stroke-affected upper limbs tend to exhibit increased co-activation of shoulder abductor muscles, including the anterior, middle, and posterior deltoid muscles [15, 16, 20]. In response to these challenges, researchers have identified key rehabilitation goals for improving intermuscular coordination in stroke-affected upper limbs [17, 20]: (1) modifying synergy vectors to reduce the coupling of the shoulder abductor muscles, (2) adjusting the activation profiles of stroke-affected synergies, and (3) modifying both synergy vectors and associated activation profiles.

Rehabilitating abnormal muscle synergy patterns poses significant challenges due to the complex and unconscious nature of human motor control [17, 22, 23]. Effective rehabilitation requires methods that can intuitively facilitate the simultaneous coordination of multiple muscle activations. Previous studies have effectively utilized myoelectric feedback to modify muscle synergy vectors and reduce undesirable co-activation post-stroke, although its application has primarily focused on decoupling muscles pairs [24–26]. Additionally, interventions combining movement exercises with robotic assistance and functional electrical stimulation have shown efficacy in indirectly altering abnormal muscle synergies and improving motor functions [17, 23, 27]. Despite these advancements, directly modifying the activation profiles without causing unintended changes in synergy vectors remains challenging, partly because it requires adjusting the timing of coordinated activation patterns involving a large number of muscles. Moreover, direct myoelectric feedback can become increasingly complex when training multiple coordinated muscle activations, as it requires users to consciously control individual muscles. Therefore, there is a necessity for methods that provide intuitive feedback to train the coordinated activation of multiple muscles.

To address these challenges, we propose an intuitive intervention paradigm termed “muscle-to-action mapping.” This approach maps desired muscle activity patterns to specific actions, such as movement or endpoint force of a limb. Unlike traditional myoelectric feedback, which requires participants to consciously adjust individual muscle activations, muscle-to-action mapping enables them to engage a target synergy activation

pattern by modulating an action-based target. Muscle-to-action mapping-based training begins by establishing the desired changes in synergy vectors or activation profiles of the stroke-affected muscle synergies. A biomechanical simulation model estimates an output kinematic or kinetic action generated by the activation of specific muscle synergies, creating an action-based target that participants use for training. These estimated action patterns serve as intuitive training targets that can be easily visualized. With muscle-to-action mapping-based guidance, stroke survivors can learn to adjust their muscle synergies by mimicking specific actions rather than consciously controlling individual muscle activations. Given the redundancy in the human musculoskeletal system, constraining upper limb postures during reaching movements is necessary to effectively induce the target muscle activation pattern.

The current study aimed to develop a force-tracking training system based on muscle-to-action mapping for improving neuromuscular coordination, specifically designed for modifying abnormal synergy activation profiles during isokinetic upper limb movements post-stroke. The training system employs a game interface where participants modulate their upper limb synergies by tracking a three-dimensional endpoint force direction, guided by a biomechanical model that predicts endpoint force based on muscle activation and limb posture. The efficacy of this system was evaluated in a study involving eleven chronic stroke survivors over 18 training sessions, assessing changes in muscle synergy vectors, activation profiles, endpoint force control, and clinical evaluation scores.

Methods

Participants

Eleven adults who had experienced chronic stroke participated in this study. The stroke survivors were screened based on the following inclusion criteria: (1) ages ranging

from 20 to 65 years, (2) hemiplegia in the upper limb, (3) absence of concurrent neurologic or orthopedic conditions besides stroke, and (4) adequate ranges of motion in the more-affected limb to execute experimental tasks (shoulder flexion: 45 degrees; shoulder abduction: 40 degrees; elbow extension: 40 degrees). Experienced occupational and physiotherapists assessed clinical motor impairment of the participants’ more-affected upper limbs using the Fugl-Meyer Assessment of upper extremity (FMA-UE, [28]). Based on the FMA-UE scores, the stroke survivors were categorized into mild (FMA-UE: 51 or above out of 66), moderate (from 31 to 50), and severe (30 or below) impairment groups. Demographic details of the participants are provided in Table 1. This study was approved by the institutional review boards of Korea Advanced Institute of Science and Technology (KH2020-180) and National Rehabilitation Center of South Korea (NRC-04-036). Prior to participant recruitment, this study was registered in the Clinical Research Information System (CRIS) of Korea National Institute of Health (KCT0005803). All recruited participants provided informed consent for their voluntary participation in this study.

Targeting stroke-specific muscle synergies

The proposed training aimed to target the stroke-specific co-activation of upper limb muscle synergies. According to our latest publications [20, 21], we observed that when matched to five synergies, the dominant limbs of neurologically intact people and the more-affected limbs of chronic stroke survivors manifested comparable synergy vectors but different activation profiles under isokinetic conditions while pushing or pulling a handle at a constant speed in six orthogonal directions in a three-dimensional space. This observation suggests that although the upper limb muscles are used in similar combinations post-stroke, there are differences in the activation timing and magnitude (Fig. 1). Our analysis revealed five muscle

Table 1 Participant demographics

Severity of motor impairment	Mild	Moderate	Severe
Number of subjects	4	3	4
Sex	2 Male, 2 Female	2 Male, 1 Female	4 Male
Months after onset of stroke	Mean: 32 SD: 40 Range: 8–92	Mean: 39 SD: 31 Range: 9–70	Mean: 99 SD: 51 Range: 30–151
Affected arm	3 Left, 1 Right	1 Left, 2 Right	2 Left, 2 Right
FMA-UE (out of 66)	Mean: 56 SD: 4 Range: 52–60	Mean: 41 SD: 4 Range: 38–45	Mean: 23 SD: 5 Range: 17–29

This table summarizes the demographic details of participants, organized into groups according to severity of motor impairment
SD: standard deviation

synergies underlying the coordination of thirteen muscles related to shoulder and elbow movements: elbow flexor (EF), elbow extensor (EE), shoulder flexor/abductor (SF/Ab), shoulder extensor/abductor (SE/Ab), and shoulder flexor/adductor (SF/Ad). Notably, the stroke-affected upper limbs exhibited two distinct synergy co-activation patterns: EF with shoulder abductor (SF/Ab or SE/Ab) synergy, and EE with SF/Ad synergy. The abnormalities observed in synergy activation profiles led to abnormal correlations between the orthogonal components of the three-dimensional endpoint force vector. This observation was manifested as coupling (i.e., a three-dimensional force generation along unintended directions due to simultaneous appearance of one-dimensional force components) among anterior, medial, and inferior forces, as

well as coupling among posterior, lateral, and superior forces [21].

The training tasks were designed to practice combinations of upper limb muscle synergies present in neurologically intact individuals to counteract the stroke-specific co-activations of the muscle synergies while reaching in six orthogonal directions. To define these targets, we first identified the essential synergy for each movement as the primary synergy required to execute the reaching task in both neurologically intact individuals and stroke survivors (e.g., elbow extension to reach anteriorly; Table 2) [20, 21]. In neurologically intact individuals, a control-specific synergy was consistently co-activated with the essential synergy to refine movement and ensure force production aligned with the intended direction. In

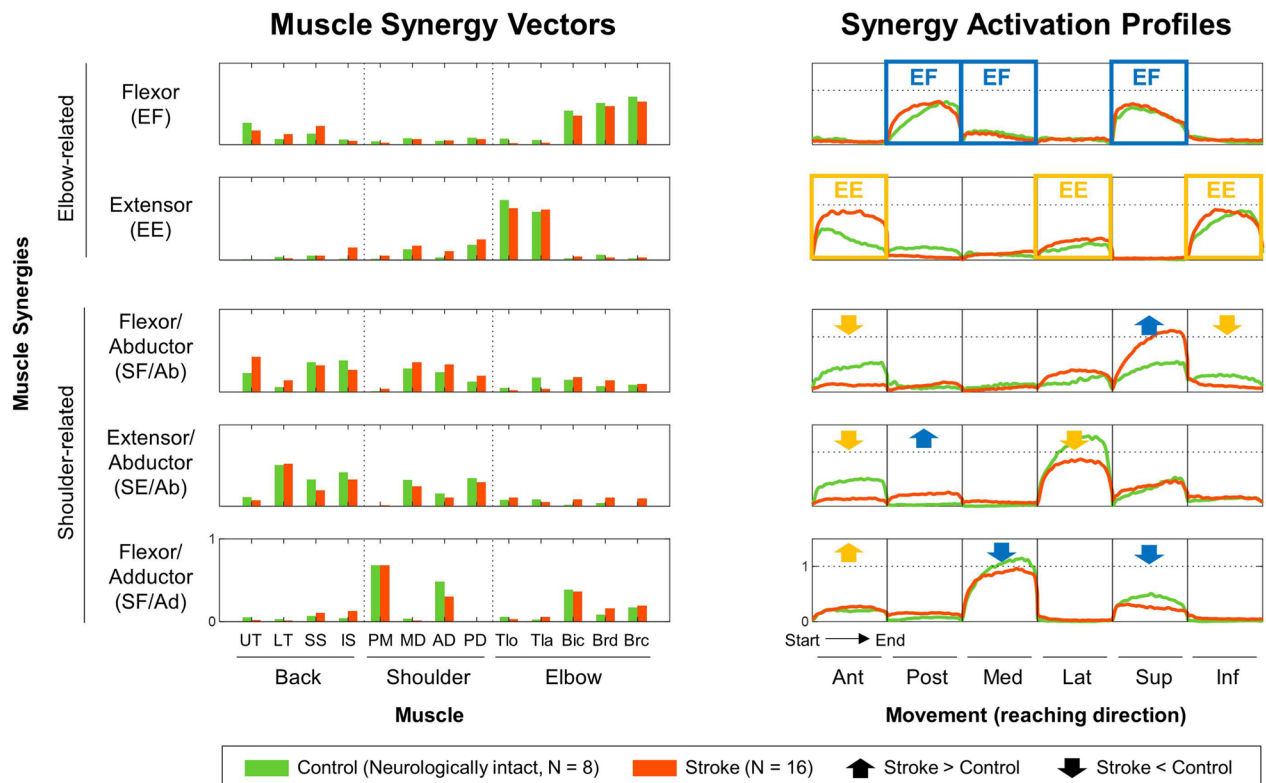


Fig. 1 Muscle synergies underlying coordination of shoulder and elbow-related muscles during isokinetic reaching (reproduced from [20]). The figure illustrates the mean muscle weights of muscle synergy vectors and the mean activation profiles for each group, encompassing six reaching movements executed in a seated posture. Yellow boxes denote activation of the elbow extensor (EE) synergy during anterior, lateral, and inferior movements, while blue boxes denote activation of the elbow flexor (EF) synergy during posterior, medial and superior movements. Upward arrowheads represent increased activation of the shoulder-related (SF/Ab, SE/Ab and SF/Ad) muscle synergies in the stroke group compared to the controls, whereas the downward arrowheads represent decreased activation of those synergies. In the more-affected upper limbs of the stroke survivors, the shoulder abductor (SF/Ab and SE/Ab) synergies were activated less during elbow extension, while activation of the shoulder adductor (SF/Ad) synergy increased. On the other hand, activation of the SF/Ab and SE/Ab synergies increased, or activation of the SF/Ad synergy decreased during the movements involving elbow flexion. UT: upper trapezius; LT: lower trapezius; SS: supraspinatus; IS: infraspinatus; PM: pectoralis major; MD: middle deltoid; AD: anterior deltoid; PD: posterior deltoid; Tlo: long head of triceps brachii; Tla: lateral head of triceps brachii; Bic: biceps brachii; Brd: brachioradialis; Brc: brachialis; Ant: anterior; Pos: posterior; Med: medial; Lat: lateral; Sup: superior; Inf: inferior

Table 2 Selection of target control-specific muscle synergies

Movement direction	Essential synergy activation	Control-specific synergy activation
Anterior	EE	SF/Ab
Posterior	EF	SF/Ad
Medial	SF/Ad	EF
Lateral	SF/Ab and SE/Ab	EE
Superior	EF	SF/Ad
Inferior	EE	SE/Ab

The essential synergy activation and control-specific synergy activation that oppose the stroke-specific co-activation patterns of the muscle synergies are listed for each movement direction

contrast, stroke participants exhibited a stroke-specific synergy, which was co-activated with the essential synergy instead of the control-specific synergy, leading to unintended force misalignment. To address this, our training approach aimed to restore more functional synergy activation patterns by promoting the activation of the control-specific synergy. By reinforcing its co-activation with the essential synergy, we sought to counteract stroke-specific co-activations and improve force direction control during reaching tasks.

Muscle-to-action mapping-based training of abnormal synergy activation profiles

To intuitively guide participants toward activating the target muscle synergies, a biomechanical model was used to map synergy activation patterns onto specific endpoint force directions during reaching tasks. These force directions were displayed as visual targets, allowing participants to modulate their force output and engage the desired synergy activation pattern without consciously controlling individual muscle activations.

According to the proposed muscle-to-action mapping-based training scheme for stroke-affected intermuscular coordination (Fig. 2), force-guidance was implemented by mapping the control-specific synergy activation onto a cursor position representing endpoint force direction. Since upper limb motion was constrained to straight-path reaching at a constant speed (i.e., isokinetic condition), endpoint force was used to guide the muscle activations. Participants were instructed to modulate the endpoint force at the handle toward the target direction, thereby intentionally deviating from their habitual muscle activation patterns and activating the target muscle synergy.

The target force direction was obtained by predicting the endpoint force generated by the activation of the

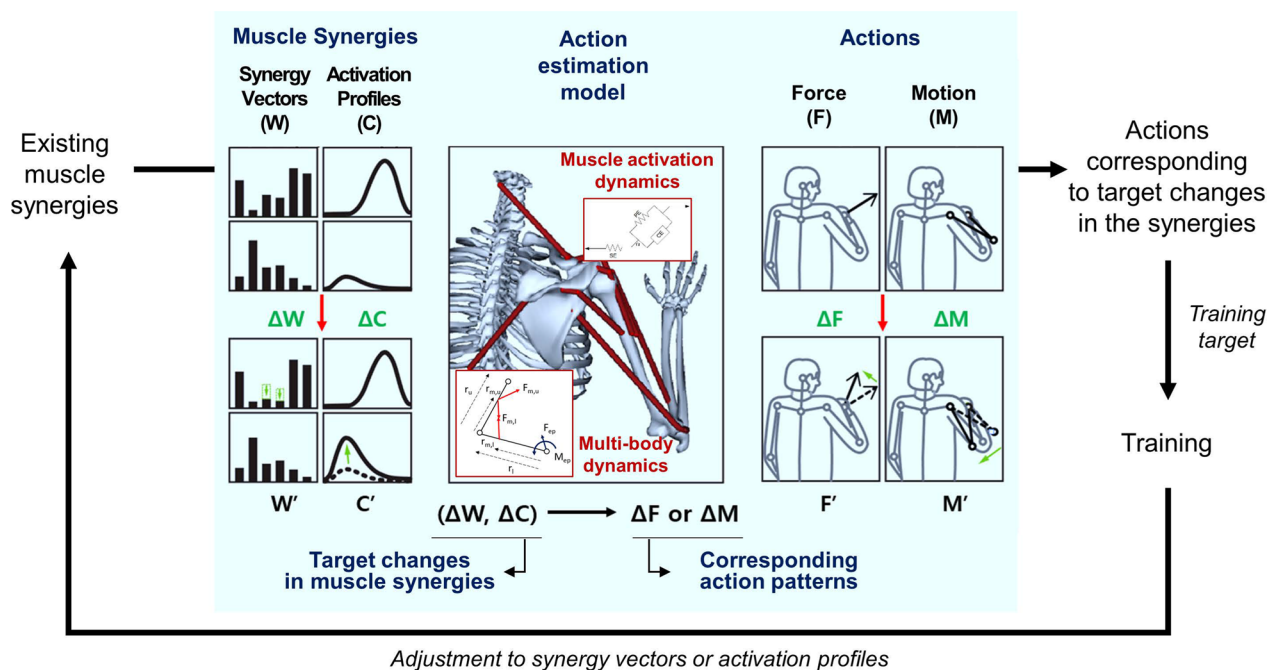


Fig. 2 Scheme of muscle-to-action mapping-based training of abnormal muscle synergies after stroke. Based on an analysis of existing muscle synergies in the more-affected limb, target changes in muscle synergy vectors (ΔW) or activation profiles (ΔC) are configured. These target changes in muscle synergies are utilized in a biomechanical model to estimate target action patterns, such as endpoint force (ΔF) or joint rotations (ΔM). The resultant actions (F' or M'), obtained by adding the estimated changes in actions to habitual (i.e., pre-training, F or M) actions, are assigned as training tasks. Following a specific period of training, the modified muscle synergies are evaluated to update the target changes in muscle synergies

dominant muscles of the target control-specific muscle synergy using a biomechanical simulation model. The target endpoint force direction (\vec{F}_{ig}) was obtained by summing directions of the habitual endpoint force during the movement (\vec{F}_{hab}) and the endpoint force generated by activation of the target muscle synergy (\vec{F}_{syn}) using Eq. 1,

$$\vec{F}_{ig}(t) = \left(\vec{F}_{hab}(t) + \alpha \times \vec{F}_{syn}(t) \right) / \left\| \vec{F}_{hab}(t) + \alpha \times \vec{F}_{syn}(t) \right\| \quad (1)$$

where the weighting factor α represented the level of difficulty of training. Setting of higher α requires larger activation of the target muscle synergy during reaching to match the force target. \vec{F}_{hab} was measured from baseline reaching movements prior to each training session, while \vec{F}_{syn} was estimated as the force direction generated by two dominant muscles (i.e., muscles of the largest muscle weights) of the target synergy. For details of the estimation model, see Additional File 1. The resultant endpoint force direction was obtained by summing the estimated forces of these two muscles, each weighted by their respective muscle weights from the mean neurologically intact muscle synergies.

In the preliminary round of clinical trials, one participant from each of the mild, moderate, and severe impairment groups (S001–3) was recruited to check potential differences in the estimation of \vec{F}_{syn} which might arise depending on the severity of motor impairment. To create individual force prediction models, endpoint force, electromyography (EMG), and kinematic data were obtained during the isokinetic reaching tasks in the six orthogonal directions prior to the training. To validate the individual force prediction models, the endpoint force was estimated from the collected EMG and kinematic data and compared with actual force data. The force prediction performance was evaluated in terms of uncentered determinant and correlation coefficients (r^2 and ρ , respectively). The individualized model could estimate the actual endpoint force within an acceptable error range of $r^2 = 0.918 \sim 0.959$ and $\rho = 0.952 \sim 0.979$ (anterior–posterior force), $0.934 \sim 0.986$ (medial–lateral force), and $\rho = 0.906 \sim 0.968$ (superior–inferior force). The detailed results are summarized in Additional File 1. Prediction of \vec{F}_{syn} was comparable across the models, and subsequent training utilized the representative model for each impairment group member. Although \vec{F}_{syn} exhibited deviations as upper limb postures changed during reaching, the mean force directions predicted for each training condition using the three individual models are illustrated in Fig. 3 for the sake of simplicity.

Training setup and protocol

An end-effector type apparatus, as proposed in ref. [29], was utilized for implementing isokinetic reaching movements in both the proposed force tracking training and the muscle synergy assessment (Fig. 4A). The apparatus employed a linear actuator to constrain the handle, ensuring its movement at a constant speed along a straight line. A six degrees of freedom force/torque sensor was integrated with the handle and collected three-dimensional endpoint force. Participants performed the isokinetic reaching movements by pushing or pulling the force-sensing handle along the linear actuator. The actuator was capable of three-dimensional rotation, thereby enabling upper limb movements in the six orthogonal directions. During both assessment and training sessions, EMG signals were collected for the muscle synergy assessment and real-time monitoring of muscle activation, respectively. Eight wireless EMG electrodes (Quattro, Delsys Inc., MA, USA) were placed on the bellies of the following muscles: (1) biceps brachii; (2) brachioradialis; (3, 4) long and lateral heads of triceps brachii; (5–7) middle, anterior, and posterior heads of deltoid; (8) clavicular head of pectoralis major. For each repetition of the reaching movements, the default reaching distance was set at 200 mm. However, if a participant could not reach the 200 mm distance, it was adjusted accordingly. Initial hand positions are illustrated in Fig. 4B.

Two user interfaces were developed for visual feedback of the participants' training performance: one for the experimenter and another for the participants (Fig. 4C). The experimenter's interface facilitated the setup of training parameters (such as movement direction, target synergy, reaching distance, difficulty, and training time) and enabled the real-time monitoring of both EMG and endpoint force signals. Experimenters used this interface to monitor live EMG signals and provide verbal feedback to ensure participants correctly activated the target synergies while minimizing stroke-specific synergy co-activations. The participant's interface provided visual feedback on the actual direction of three-dimensional endpoint force (i.e., a force cursor), alongside the target force direction (i.e., a force target). Participants used this interface to align the force cursor with the force target by modulating the endpoint force direction. Additionally, a force magnitude display was incorporated to encourage the participants to gradually adjust muscle activation while maintaining the endpoint force magnitude within a training session.

The training protocol encompassed 18 training sessions, each lasting 25 min (excluding breaks) conducted over three weeks with six sessions per week (i.e., one to two sessions per day). Additionally, pre- and post-training assessment sessions were included to evaluate

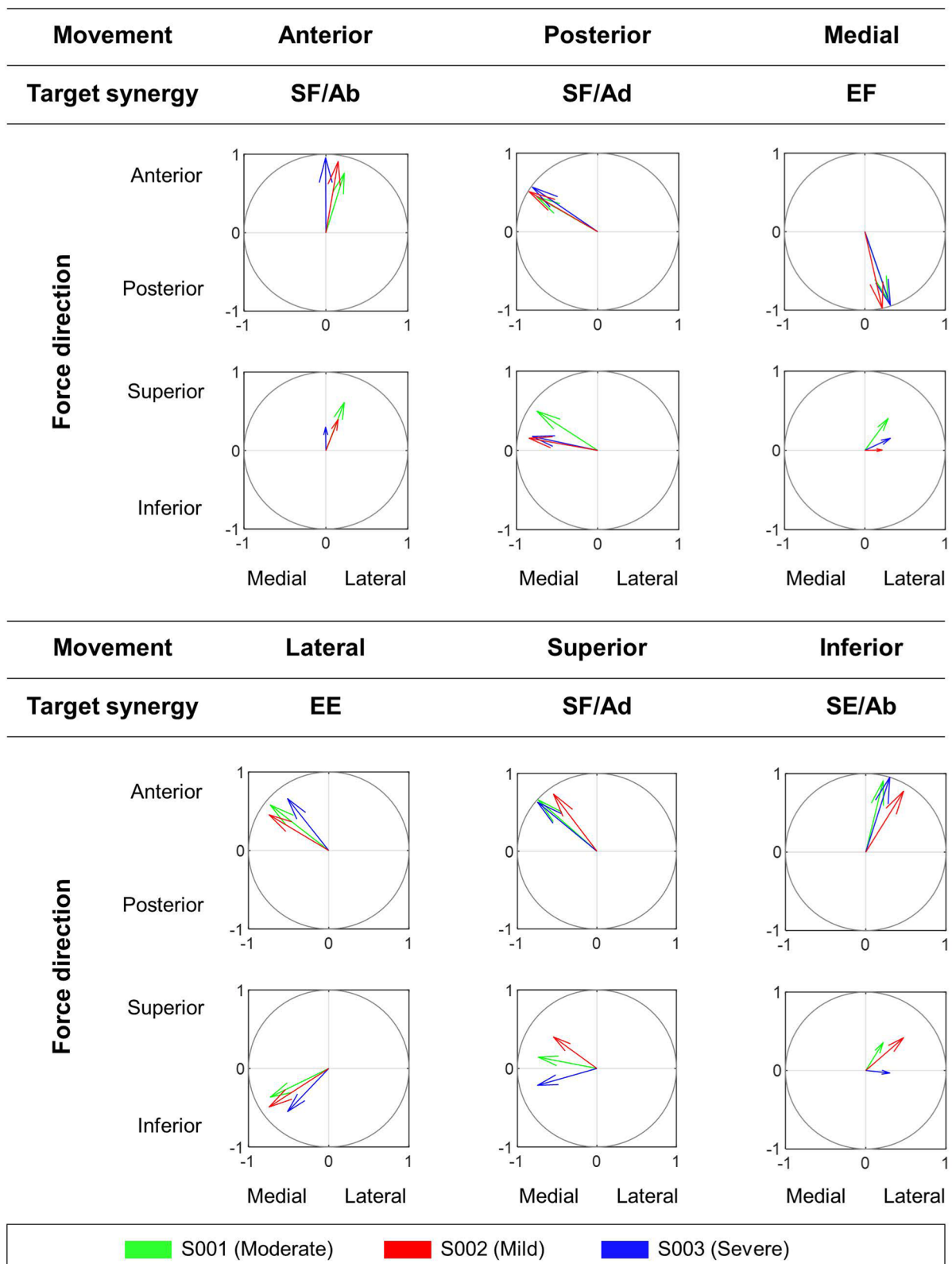


Fig. 3 Endpoint force directions predicted from the control-specific synergies activations for six training conditions. The top row includes training based on reaching movements in anterior, posterior, and medial directions, while the bottom row includes training focused on lateral, superior, and inferior movements. For each movement, the upper graph depicts endpoint force direction in the anterior–posterior and medial–lateral plane. The lower graph illustrates the force direction in the superior–inferior and medial–lateral plane

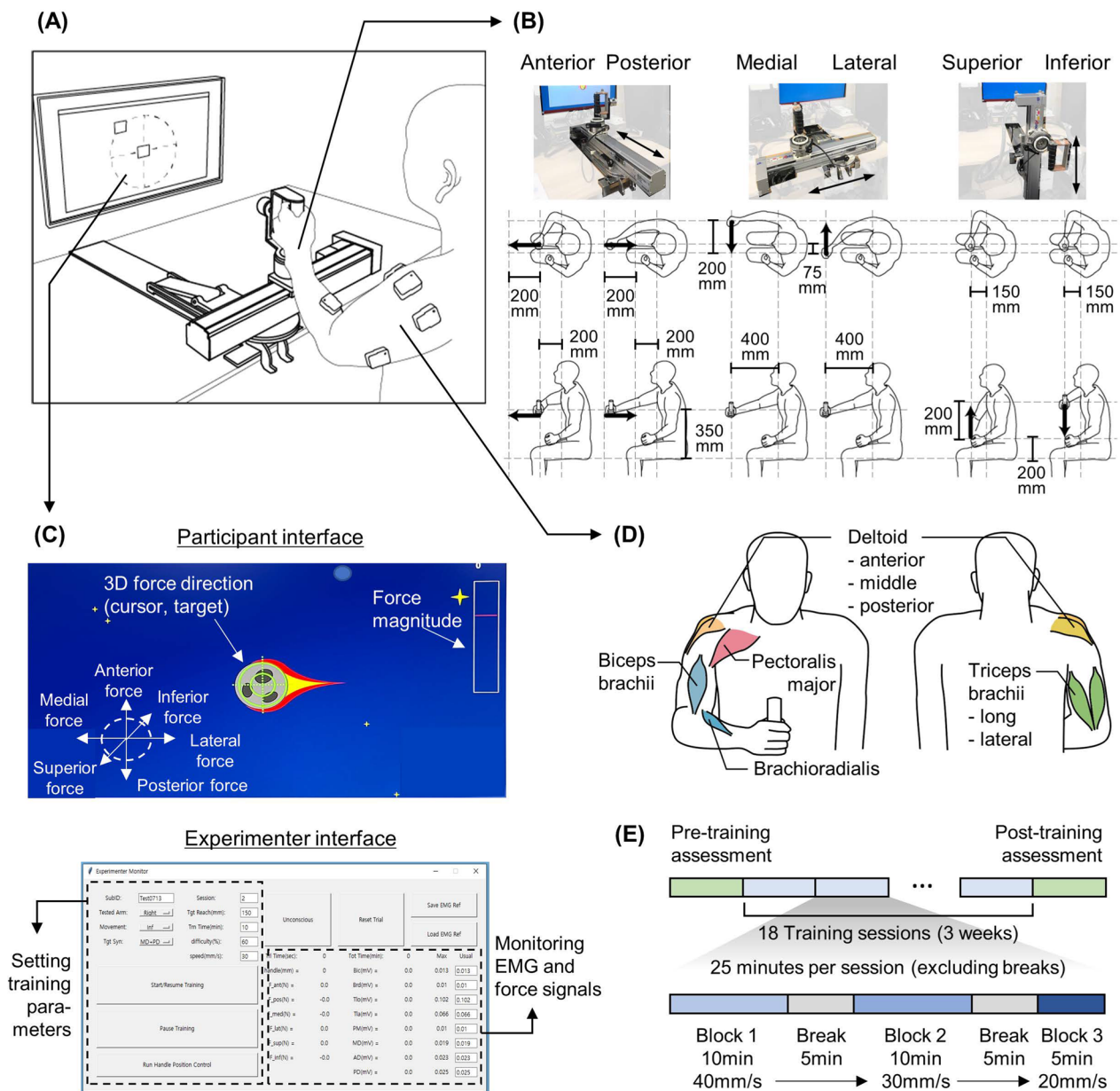


Fig. 4 Training setup and protocol. **A** Training setup consists of three components: a mechanical apparatus for implementing isokinetic reaching movements, training interfaces, and EMG sensors. **B** The mechanical apparatus features a force-sensing handle that moves along a linear actuator. The actuator was rotated in a three-dimensional space to implement reaching movements in the six orthogonal directions (anterior, posterior, medial, lateral, superior, and inferior directions). For each movement direction, the initial and final positions of the handle were aligned with the participant. **C** Two training interfaces were developed. The participant interface provided visual feedback on the three-dimensional endpoint force direction. The participant modulated a force cursor (e.g., represented as a crosshair) by controlling the endpoint force direction to hit a force target (e.g., a meteor). During training, the experimenter set parameters to configure a training task, monitored EMG and endpoint force signals in real-time, and provided verbal instructions. **D** EMG signals were collected from eight major muscles involved in shoulder and elbow movements. **E** A participant underwent 18 training sessions and two assessment sessions—pre- and post-training—for three weeks. Each training session was divided into three blocks, varying in training time (5–10 min), and reaching speed (20–40 mm/s). In subsequent blocks, the training was conducted at slower speeds to increase intensity, as participants had to maintain the endpoint force direction for a longer time while reaching the same distance. After completing each block, a five-minute break was given

upper limb muscle synergies and endpoint force control (Fig. 4E). During the assessment sessions, participants performed isokinetic upper limb movements for six repetitions in each of the six orthogonal directions. They were instructed to generate the maximum endpoint force strictly along the movement directions, reaching a distance of 200 mm at a speed of 30 mm/s. No force or EMG feedback was provided during the assessment sessions to objectively assess participants' ability to execute the reaching tasks independently after training. Only the reaching distance was displayed on the screen. In addition to the biomechanical evaluations, experienced occupational and physiotherapists assessed clinical outcomes of the proposed training using the FMA-UE score and the functional ability scale of Wolf Motor Function Test (WMFT-FAS, [30]).

For each training session, the experimenter assigned movement in one of the six orthogonal directions based on the severity of abnormal force control observed during pre-assessment. Consequently, participants without abnormal force coupling in a specific direction did not receive training for that directional movement. Table 3 summarizes the number of training sessions in each reaching direction. Each training session was structured into three blocks. To progressively elevate the difficulty and duration of the target muscle synergy activation, the movement speed decreased in each subsequent block as follows: in Block 1, 40 mm/s; in Block 2, 30 mm/s; and in Block 3, 20 mm/s. A slower movement speed made it more difficult to complete the force tracking training, requiring participants to maintain the endpoint force for longer durations. Therefore, the first two blocks lasted ten minutes each, with the third block lasting five

minutes. A five-second break followed each repetition, and a five-minute break was given after completing each block. All participants were able to complete the training using breaks as needed, except in one instance where a participant was unable to adhere to the training protocol in one direction, leading to the omission of that directional data from the analysis.

Data analysis

Muscle synergies underlying the activation of the eight elbow and shoulder muscles were identified through non-negative matrix factorization (NNMF, [31]). Prior to NNMF analysis, the EMG signals were denoised using band-rejection (5th-order Butterworth, cut-off: 55–65 Hz), low-pass (5th-order Butterworth, cut-off: 450 Hz), and high-pass (3rd-order Butterworth, cut-off: 30 Hz) filters [32]. The filtered signal was demeaned by subtracting the median value. The EMG envelope was obtained by applying a low-pass filter (5th-order Butterworth, cut-off: 1 Hz) after full-wave rectification. Finally, the mean value of the EMG envelope during the baseline period was subtracted. The processed EMG data were resampled using linear interpolation to match 4000 data points across trials, concatenated across trials, and normalized by the maximum value of each muscle. To determine the appropriate number of muscle synergies, we applied the same synergy selection criteria as in our previous study [20]. This step was taken to confirm whether stroke participants in the current study exhibited a similar number of synergies as those in our prior study before standardizing the synergy number for further analysis. NNMF was repeated 100 times, and the solution with the highest

Table 3 The number of training sessions in each direction

Participants	Group	Movements assigned for training					
		Ant	Post	Med	Lat	Sup	Inf
S001	Moderate	6	–	–	6	6	–
S002	Mild	8	–	2	8	–	–
S003	Severe	5	1	1	1	5	5
S004	Mild	1	10	–	1	–	6
S005	Severe	5	2	2	5	2	2
S006	Severe	7	3	–	3	2	3
S007	Mild	–	10	–	4	–	4
S008	Mild	3	8	–	4	–	3
S009	Moderate	–	–	4	4	10	–
S010	Severe	3	3	3	3	3	3
S011	Moderate	4	4	–	10	–	–

The number of training sessions for each movement direction is listed per participant. Although the total training dosage was 18 sessions, the frequency per direction was assigned based on the pre-assessment results

Ant: anterior; Post: posterior; Med: medial; Lat: lateral; Sup: superior; Inf: inferior

variance accounted for (VAF) was selected as the optimal decomposition to ensure robustness.

To quantify changes in intermuscular coordination induced by the training, we first evaluated the similarity of synergy vectors between pre- and post-training conditions. The pre- and post-training muscle synergies were matched to reference synergies (EE, EF, SF/Ab, SE/Ab, and SF/Ad) based on the lowest squared difference between the synergy vector weights. The similarity of a pair of synergy vectors was then determined as the cosine similarity of corresponding synergy vectors between the pre- and post-training muscle synergy sets. The mean similarity values derived from the muscle synergy vector sets were compared to a threshold representing similarity by chance, which was established using sets of five random vectors sampled from the pre- and post-training EMG data. A similarity value of 0.79 was determined as the 95th percentile threshold; any similarity exceeding this value would indicate that the pre- and post-training synergy vectors could be considered highly similar. For a comprehensive description of this methodology, including the detailed process of generating EMG-based random vectors and determining the similarity threshold, please refer to our previous publication [20].

A synergy activation score was created to evaluate the activation of the desirable muscle synergies influenced by the training as shown in Eq. (2). The mean area under the activation profiles of the target and essential synergies (A_{tar} and A_{ess} , respectively) was multiplied by the training dosage in that direction divided by the total number of training sessions ($\frac{X_{dosage}}{18}$). This approach eliminated synergy activation scores for untrained movement directions, allowing us to focus solely on changes due to the training. Multiplying the scores by the dosage emphasized the directions that were trained more intensively and naturally excluded scores for untrained directions (where dosage=0). This resulted in six scores, one for each movement direction. Due to the variability in training dosages among participants, we averaged these six scores for each participant, facilitating a more standardized comparison of the overall training effect. The synergy activation score ranged from 0 to 100.

$$Synergy\ Activation\ Score = \left(\frac{A_{tar} + A_{ess}}{2} \right) * \frac{X_{dosage}}{18} \quad (2)$$

The control of three-dimensional endpoint forces pre- and post-training was evaluated by a force control score as shown in Eq. (3). The area under the force curve in the target direction (F_{tar}) was rewarded while the area under forces in the other two orthogonal directions (F_{nontar}) were penalized. This index was designed to assess the changes in undesired force coupling due to the training.

Similar to the activation score, the training dosage ratio in the respective direction ($\frac{X_{dosage}}{18}$) was multiplied, and the mean directional scores of each participant was calculated. The force control score ranged from -100 to 100 . Additionally, the association between the changes in synergy activation and force control was assessed by examining the correlation between the changes in the scores after training.

$$Force\ Control\ Score = \left(F_{tar} - \frac{\sum F_{nontar}}{2} \right) * \frac{X_{dosage}}{18} \quad (3)$$

The changes in clinical assessment scores were evaluated using the FMA-UE and the WMFT-FAS. To explore the relationship between the modifications in muscle synergy activation profiles and specific clinical outcomes, we searched for strong correlations (defined as over 0.7) between the synergy activation scores and clinical sub-scores.

The Wilcoxon Signed-Rank Test was used to compare the medians of synergy activation, force control, and clinical assessment scores pre- and post-training. Additionally, Pearson's correlation coefficient was used to assess the correlation between the changes in synergy activation scores and force control scores. A significance level of 0.05 was used for all statistical tests. Statistical analyses were performed using MATLAB.

Results

Muscle synergy composition and activation profiles

From the NNMF analysis, among the 11 subjects, 8 exhibited 4 synergies, 2 exhibited 5 synergies, and 1 exhibited 6 synergies, yielding a mean of 4.36. These findings closely align with our previous study, which included 16 subjects, where 11 had 4 synergies, 4 had 5 synergies, and 1 had 6 synergies, with a mean of 4.38 [20]. Following our previous methodology, we standardized synergy extraction to five synergies and confirmed that the synergy vectors in the stroke participants remained comparable to those of controls (Fig. 1).

From the NNMF analysis, five muscle synergies were obtained to account for a majority of EMG variance (VAF: 0.98 ± 0.01 ; mean \pm standard deviation). Additionally, the percent change in VAF from pre- to post-training for five muscle synergies was less than 1%, confirming that the number of synergies remained stable throughout the intervention. Figure 5 shows a representative set of the muscle synergy vector similarity, activation scores, and force control scores collected from a single participant. The synergy activation scores across all participants pre- and post-training (7.87 ± 3.29 and 9.12 ± 3.64 , respectively) showed a statistically significant increase ($p < 0.05$) in the desired muscle synergy activations following the

intervention (Fig. 6A). The synergy vectors had a mean similarity of 0.87 ± 0.1 , which exceeded the threshold value of 0.79. This indicates that the training did not substantially alter the composition of the muscle synergy vectors (Fig. 6B). This consistency in muscle synergy vectors suggests that only the activation profiles of synergy vectors were primarily influenced by the intervention.

Force control

The analysis of the mean force control scores revealed a statistically significant reduction ($p < 0.01$) in abnormal force couplings during reaching tasks (Fig. 6C). This pre- to post-training improvement from 19.47 ± 12.2 to 23.73 ± 12.65 suggests that participants learned to better direct their forces towards the targets, thus reducing unintentional force generation in non-target directions after the isokinetic exercise. The relationship between improvements in synergy activation and force control was also observed (Fig. 6D). A strong correlation ($r = 0.85$, $p < 0.01$) indicated a statistically significant link between the two training outcomes. Notably, this correlation was independent of the participants' stroke impairment severity, highlighting the intervention's efficacy across various degrees of motor impairment after stroke.

Clinical evaluations

Clinical evaluations using the FMA-UE and WMFT-FAS provided robust evidence of the observed functional improvements. The FMA-UE scores demonstrated a statistically significant increase, averaging 3.36 ± 2.8 ($p < 0.01$; Fig. 6E), while the WMFT-FAS scores exhibited an even more pronounced statistically significant enhancement, with a mean increase of 6.45 ± 4.78 ($p < 0.01$; Fig. 6F). Furthermore, the changes in activation scores showed a strong correlation ($r = 0.76$) with the WMFT-FAS item "6. Hand to box," a task that closely mirrors the forward-reaching movements emphasized in the training. In contrast, other clinical sub-scores

exhibited moderate to low correlations ($r = 0-0.66$) with changes in activation scores.

Discussion

The current study introduced a muscle-to-action mapping approach to improve motor control by modifying the activation profiles of abnormal stroke-affected muscle synergies. We developed a force-tracking, rehabilitation training system that used muscle-to-action mapping to test whether desired muscle activity patterns can be induced in chronic stroke survivors by generating the corresponding endpoint force in three-dimensional space. The intervention significantly increased the magnitude of targeted muscle synergy activations and improved endpoint force control during isokinetic reaching. These results confirm that muscle-to-action mapping is an effective and intuitive method for altering muscle synergy activation profiles, leading to both functional and clinical improvements in chronic stroke survivors.

By integrating muscle-to-action mapping into isokinetic exercises, we built upon our prior research that identified a positive link between stroke-affected upper limb muscle synergies and abnormal endpoint force control [20, 21]. Unlike traditional force feedback training methods, our approach utilized a biomechanical model to establish force targets corresponding to specific muscle synergies. By mapping these intermuscular coordination patterns to actions that are intuitive to follow, this approach successfully addressed the challenge of simultaneously providing live feedback recorded from multiple muscles [22]. To navigate motor redundancy—where multiple muscle activation solutions can achieve the same force output—our training sessions adhered to strict postural guidelines while monitoring real-time EMG signals. By imposing kinematic constraints to narrow the solution space and providing verbal feedback based on real-time EMG monitoring, we were able to reliably induce the desired synergy activation profiles while maintaining consistent synergy vectors as intended.

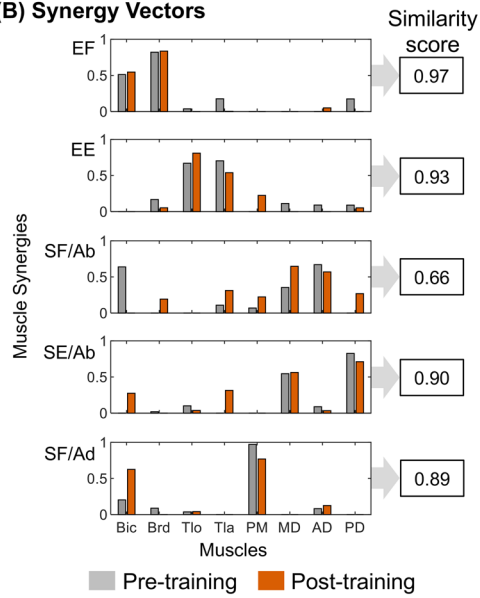
(See figure on next page.)

Fig. 5 Example of training program, muscle synergy vectors, activation profiles, and endpoint forces pre- and post-training for one participant. Attributes of muscle synergies pre- and post-training are depicted in grey and orange, respectively. **A** Training program assigned to one participant with moderate severity. The table outlines the training movements and corresponding dosage, essential synergies, and control-specific synergies. **B** Muscle synergy vectors from the pre- and post-training assessment. The weight similarity scores for each synergy are shown on the right. **C** Synergy activation profiles from the pre- and post-training assessment. The essential and control-specific synergies are outlined in blue and green, respectively, for each of the trained directions. Arrows depict increases or decreases in activation levels of each synergy. The synergy activation scores for each of the trained movement directions are shown on the bottom, and the collective mean score is shown to the right. **D** Endpoint forces from the pre- and post-training assessment. The target and non-target directions are outlined in green and red, respectively, for each of the trained directions. Arrows depict increases or decreases in force of each direction. The force control scores for each movement direction are shown on the bottom, and the collective mean score is shown to the right. Bic: biceps brachii; Brd: brachioradialis; Tlo: long head of triceps brachii; Tla: lateral head of triceps brachii; PM: pectoralis major; MD: middle deltoid; AD: anterior deltoid; PD: posterior deltoid; Ant: anterior; Post: posterior; Med: medial; Lat: lateral; Sup: superior; Inf: inferior

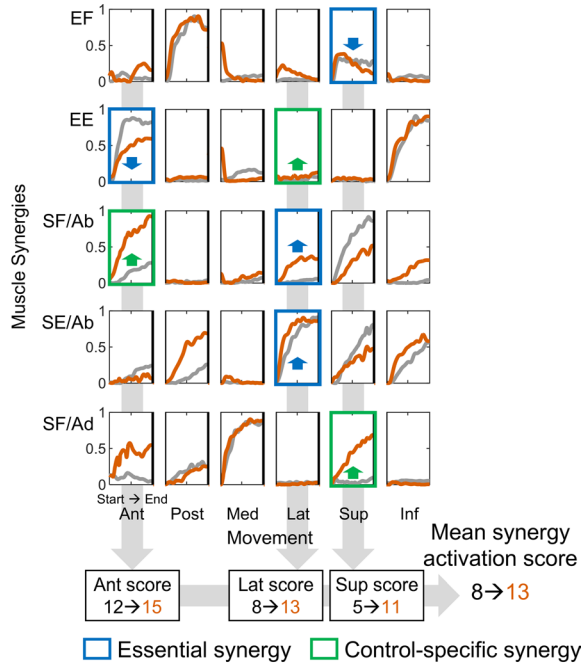
(A) Training Program

Movement	Dosage	Essential synergy	Control-specific synergy
Anterior	6 sessions	EE	SF/Ab
Lateral	6 sessions	SF/Ab and SE/Ab	EE
Superior	6 sessions	EF	SF/Ad

(B) Synergy Vectors



(C) Synergy Activation Profiles



(D) Endpoint Forces

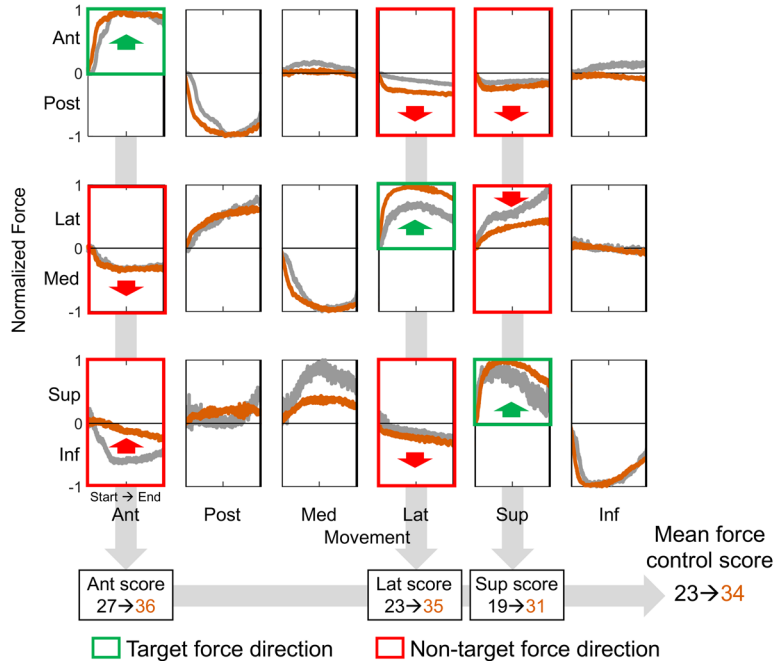


Fig. 5 (See legend on previous page.)

The improvements in synergy activation scores from the intervention underscored the efficacy of the training to induce desired muscle synergy activation profiles through the muscle-to-action mapping. Additionally, the muscle synergy analysis revealed that the overall structure of synergy vectors remained largely unchanged post-training. The preservation of synergy structure aligns with the concept of hard-wired muscle synergy [5], that the synergy structure is relatively fixed within the spinal circuit [33]. Nevertheless, there remains the possibility that muscle composition of a synergy can be tuned to some extent through training as other neuroanatomical mechanisms, such as overlapping cortical representation of muscles, are also involved in synergy formation. This was evident in the studies that used myoelectric feedback to modify muscle synergy vector weights [23, 25, 26]. Our method offers a complimentary approach that can modify the activation profiles of stroke-affected synergies. Synergy activation profiles, which stem from motor planning in the brain, are considered relatively flexible and modifiable through training as we demonstrated, reflecting the neuroplasticity observed in motor learning [6, 34–37].

Furthermore, the targeted changes in synergy activation profiles were linked with functional improvements. The force control scores showed a strong correlation with the synergy activation scores, suggesting that the reduction in abnormal force coupling was associated with altered synergy activation profiles. This outcome was expected, as the control-specific synergies trained for each direction counteracted the stroke-specific co-activation patterns that induced abnormal force coupling. However, the correlation between the changes in synergy activation scores and specific clinical sub-scores was not demonstrated, possibly due to the personalized nature of the training. A strong correlation was observed only in a specific WMFT-FAS task involving forward-reaching movement, which directly mirrored the training activities. It is unclear how each muscle synergy relates to the specific sub-motor tasks of these clinical evaluations.

The concept of muscle-to-action mapping has broader potential for various designs in intermuscular coordination training. In terms of clinical outcomes, the FMA-UE

and WMFT-FAS scores improved by 3.36 and 6.45 points respectively. These results are consistent with various interventions on chronic stroke survivors, such as robot-assisted therapy, vagus nerve stimulation, and bilateral motor priming [38–41]. Although comparable in terms of clinical improvements, our approach targets different aspects of motor control, specifically the underlying neural basis of intermuscular coordination, not addressed by previous interventions. This distinction suggests additional potential for recovery by integrating various rehabilitation strategies [41]. Our method's ability to focus on specific neuromuscular adjustments offers a complementary avenue for enhancing motor recovery, making it a worthwhile addition to existing stroke rehabilitation protocols. Thus, chronic stroke survivors who have improved functionality through various rehabilitation interventions but still exhibit poor intermuscular coordination and highly coupled upper limb movement may benefit from the muscle synergy activation profile targeted training. While this study focused on chronic stroke survivors to first evaluate the feasibility of the approach, future work will explore its application in acute and sub-acute patients, where greater neuroplasticity may further enhance recovery. For stroke survivors struggling to generate sufficient endpoint force, the targeted muscle coordination pattern could be mapped onto movements in free space rather than endpoint force. Similar to mapping onto endpoint force, biomechanical simulation or data-driven estimation could be used to create target movements for training. Furthermore, to adjust the synergy vector weighting coefficient of a particular muscle within a synergy, the target action could be adjusted by shifting the associated action of the targeted synergy toward or against the action of the targeted muscle, providing a nuanced approach to rehabilitating motor function.

The study demonstrated the feasibility of using muscle-to-action mapping to train muscle synergy activation profiles, but it involved several limitations. While the overall treatment dosage was consistent, the training dosage for each movement direction was individualized to accommodate the differing impairments of each participant. Although this personalized approach helped address the specific weakness of each participant, the

(See figure on next page.)

Fig. 6 Training-induced changes in muscle synergy, force control, and clinical evaluations. Pre- and post-training conditions are shown in grey and orange, respectively. The mild, moderate, and severe impairment groups are colored in red, green, and blue, respectively. Asterisks indicate statistical significance. **A** Mean muscle synergy activation scores pre- and post-training with error bars indicating standard deviation. **B** Mean muscle synergy vector similarity scores across trained muscle synergies, with error bars indicating standard deviation. **C** Mean force control scores pre- and post-training with error bars indicating standard deviation. **D** Correlation between synergy activation and force control scores across mild, moderate, and severe impairment groups. The dotted line indicates the best fit trend line. **E** FMA-UE clinical scores pre- and post-training for mild, moderate, and severe impairment groups with dotted lines showing best fit trends for each group. **F** WMFT-FAS clinical scores pre- and post-training for mild, moderate, and severe impairment groups with dotted lines showing best fit trends for each group

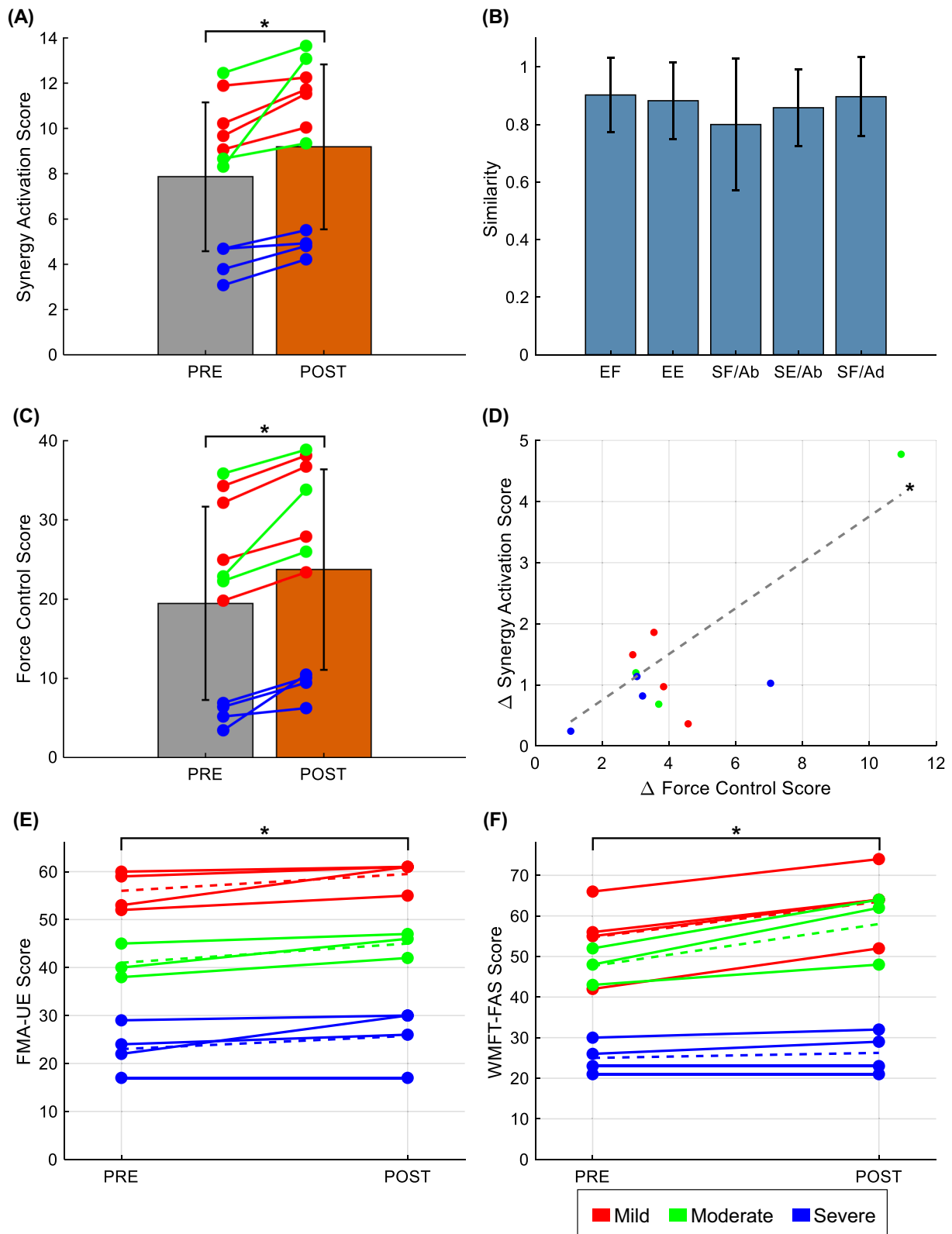


Fig. 6 (See legend on previous page.)

variability in dosages limited our ability to derive generalized insights into the efficacy of training specific synergies and movement directions. Future research should focus on these details to enhance understanding of the functions of each targeted synergy and the influence of initial impairment levels on intervention outcomes. The cohort also included participants with varying stroke severities, which may have influenced individual responsiveness to training. While this variability allowed us to assess feasibility across different severity levels, future studies should consider stratifying participants by severity to improve generalizability. Moreover, one participant was unable to follow the synergy activation profile training for a specific direction, indicating that certain synergy activations profiles may not be achievable despite repeated training attempts. Integrating supplementary coaching aspects like electrical stimulation or virtual reality could potentially aid participants in learning to activate these challenging synergies, offering a promising direction for enhancing the effectiveness of the training regimen.

Conclusion

In conclusion, this study demonstrated the feasibility of the muscle-to-action mapping method for training muscle synergy activation profiles in stroke survivors. By employing a biomechanical model to generate specific endpoint forces, the method not only effectively modified synergy activation profiles but also improved force control during reaching tasks, thereby translating neuromuscular adjustments into tangible clinical improvements. These results suggest that muscle-to-action mapping could be a valuable addition to stroke rehabilitation, offering an intuitive approach to train intermuscular coordination and enhance motor recovery.

Abbreviations

FMA-UE	Fugl-Meyer Assessment of upper extremity
WMFT-FAS	Wolf Motor Function Test functional ability scale
EF	Elbow flexor
EE	Elbow extensor
SF/Ab	Shoulder flexor/abductor
SE/Ab	Shoulder extensor/abductor
SF/Ad	Shoulder flexor/adductor
EMG	Electromyography
NNMF	Non-negative matrix factorization

Supplementary Information

The online version contains supplementary material available at <https://doi.org/10.1186/s12984-025-01630-y>.

Additional file 1. Estimation of the Target Force Directions for Upper Limb Muscle Synergies. This supplementary material aims to detail the processes for estimating actions (especially, endpoint force directions), which induce activation of specific upper limb muscle synergies. Section 1 provides an overview of force estimation, covering both simulations using a musculoskeletal model of the upper limb and the individualization of

this model based on pre-training upper limb exercise data. Section 2 and 3 describe details of the biomechanical simulation and the individualization processes, respectively. Finally, section 4 presents the estimation of force directions for each muscle synergy, utilizing individual models obtained from three chronic stroke survivors exhibiting varying levels of motor impairment.

Acknowledgements

All authors appreciate Ms. Ye-Jin Hahm for her effort to recruit the stroke survivors and manage their experiment schedule.

Author contributions

HL, J-HP, J-HS, JR, and H-SP conceived the study design. HL, J-HP, and J-HS carried out the experiment to identify muscle synergies of stroke survivors. HL and J-HP analyzed the data and drafted the manuscript with input from all other authors. J-HS, JR, and H-SP contributed to the critical revision of the manuscript. H-SP supervised the study.

Funding

This study was supported in part by the Translational Research Program for Rehabilitation Robots (#NRCTR-EX23006) at the National Rehabilitation Center, Ministry of Health and Welfare, South Korea; in part by the Technology Innovation Program (Grant No. 20014480, A light-weight wearable upper limb rehabilitation robot system and intact self-training and assessment platform customizable for individual patients), funded by the Ministry of Trade, Industry and Energy (MOTIE), South Korea; and in part by the U.S. National Science Foundation CAREER Award (#2145321 to Roh).

Availability of data and materials

The datasets used and/or analyzed during the current study are available from the corresponding author on reasonable request.

Declarations

Ethics approval and consent to participate

This study involving human participants was reviewed by the institutional review boards of the Korea Advanced Institute of Science and Technology (approval code: KH2020-180) and the National Rehabilitation Center of Korea (approval code: NRC-04-036).

Consent for publication

Not applicable.

Competing interests

HL, J-HP, J-HS, and H-SP are inventors of three patent applications (two granted and one pending in South Korea: KR102246686, KR102276625, KR1020210146546) related to the experimental apparatus and the muscle-to-action mapping training method validated in this study.

Author details

¹Department of Mechanical Engineering, Korea Advanced Institute of Science and Technology, Daejeon 34141, South Korea. ²Department of Neurorehabilitation, National Rehabilitation Center, Seoul 01022, South Korea. ³Department of Biomedical Engineering, University of Houston, Houston, TX 77004, USA.

Received: 14 August 2024 Accepted: 8 April 2025

Published: 28 April 2025

References

1. Waking JM, Blake OM, Chan HK. Muscle coordination is key to the power output and mechanical efficiency of limb movements. *J Exp Biol.* 2010;213(3):487–92.
2. Chapman AE, Sanderson DJ. Muscular coordination in sporting skills. In: Winters JM, Woo SL-Y, editors. *Multiple muscle systems*. Berlin: Springer; 1990. p. 608–20.

3. Keshner EA, Allum JHJ. Muscle activation patterns coordinating postural stability from head to foot. In: Winters JM, Woo SL-Y, editors. *Multiple muscle systems*. Berlin: Springer; 1990. p. 481–97.
4. Bizzi E, Cheung VCK. The neural origin of muscle synergies. *Front Comput Neurosci*. 2013;7:51.
5. McMorland AJC, Runnalls KD, Byblow WD. A neuroanatomical framework for upper limb synergies after stroke. *Front Hum Neurosci*. 2015;9:82.
6. Cheung VCK, Seki K. Approaches to revealing the neural basis of muscle synergies: a review and a critique. *J Neurophysiol*. 2021;125(5):1580–97.
7. Matsunaga N, Kaneoka K. Comparison of modular control during smash shot between advanced and beginner badminton players. *Appl Bionics Biomech*. 2018;2018:6592357.
8. Kim M, Kim Y, Kim H, Yoon B. Specific muscle synergies in national elite female ice hockey players in response to unexpected external perturbation. *J Sports Sci*. 2018;36(3):319–25.
9. Baifa Z, Xinglong Z, Dongmei L. Muscle coordination during archery shooting: a comparison of archers with different skill levels. *Eur J Sport Sci*. 2023;23:54–61.
10. Cheung VCK, Cheung BMF, Zhang JH, Chan ZYS, Ha SCW, Chen CY, et al. Plasticity of muscle synergies through fractionation and merging during development and training of human runners. *Nat Commun*. 2020;11(1):1–15. <https://doi.org/10.1038/s41467-020-18210-4>.
11. Vaz JR, Olstad BH, Cabri J, Kjendlie PL, Pezarat-Correia P, Hug F. Muscle coordination during breaststroke swimming: comparison between elite swimmers and beginners. *J Sports Sci*. 2016;34(20):1941–8.
12. Allen JL, Kautz SA, Neptune RR. The influence of merged muscle excitation modules on post-stroke hemiparetic walking performance. *Clin Biomech*. 2013;28(6):697–704.
13. Sukal TM, Ellis MD, Dewald J. Shoulder abduction-induced reductions in reaching work area following hemiparetic stroke: neuroscientific implications. *Exp Brain Res*. 2007;183(2):215–23.
14. Cheung VCK, Turolla A, Agostini M, Silvoni S, Bennis C, Kasi P, et al. Muscle synergy patterns as physiological markers of motor cortical damage. *Proc Natl Acad Sci USA*. 2012;109(36):14652–6.
15. Roh J, Rymer WZ, Perreault EJ, Yoo SB, Beer RF. Alterations in upper limb muscle synergy structure in chronic stroke survivors. *J Neurophysiol*. 2013;109(3):768–81.
16. Roh J, Rymer WZ, Beer RF. Evidence for altered upper extremity muscle synergies in chronic stroke survivors with mild and moderate impairment. *Front Hum Neurosci*. 2015;9:6.
17. Tropea P, Monaco V, Coscia M, Posteraro F, Micera S. Effects of early and intensive neuro-rehabilitative treatment on muscle synergies in acute post-stroke patients: a pilot study. *J Neuroeng Rehabil*. 2013;10(1):1–15.
18. Coscia M, Cheung VCK, Tropea P, Koenig A, Monaco V, Bennis C, et al. The effect of arm weight support on upper limb muscle synergies during reaching movements. *J Neuroeng Rehabil*. 2014;11(1):1–15.
19. Runnalls KD, Ortega-Auriol P, McMorland AJC, Anson G, Byblow WD. Effects of arm weight support on neuromuscular activation during reaching in chronic stroke patients. *Exp Brain Res*. 2019;237(12):3391–408.
20. Park JH, Shin JH, Lee H, Roh J, Park HS. Alterations in intermuscular coordination underlying isokinetic exercise after a stroke and their implications on neurorehabilitation. *J Neuroeng Rehabil*. 2021;18(1):1–17.
21. Park JH, Shin JH, Lee H, Roh J, Park HS. Relevance of upper limb muscle synergies to dynamic force generation: perspectives on rehabilitation of impaired intermuscular coordination in stroke. *IEEE Trans Neural Syst Rehabil Eng*. 2023;31:4851–61.
22. Hong YNG, Ballekere AN, Fregly BJ, Roh J. Are muscle synergies useful for stroke rehabilitation? *Curr Opin Biomed Eng*. 2021;19: 100315. <https://doi.org/10.1016/j.cobme.2021.100315>.
23. Lencioni T, Fornia L, Bowman T, Marzegan A, Caronni A, Turolla A, et al. A randomized controlled trial on the effects induced by robot-assisted and usual-care rehabilitation on upper limb muscle synergies in post-stroke subjects. *Sci Rep*. 2021;11(1):1–15. <https://doi.org/10.1038/s41598-021-84536-8>.
24. Mugler EM, Tomic G, Singh A, Hameed S, Lindberg EW, Gaide J, et al. Myoelectric computer interface training for reducing co-activation and enhancing arm movement in chronic stroke survivors: a randomized trial. *Neurorehabil Neural Repair*. 2019;33(4):284–95.
25. Seo G, Park JH, Park HS, Roh J. Developing new intermuscular coordination patterns through an electromyographic signal-guided training in the upper extremity. *J Neuroeng Rehabil*. 2023;20(1):1–17. <https://doi.org/10.1186/s12984-023-01236-2>.
26. Seo G, Kishta A, Mugler E, Slutzky MW, Roh J. Myoelectric interface training enables targeted reduction in abnormal muscle co-activation. *J Neuroeng Rehabil*. 2022;19(1):1–12. <https://doi.org/10.1186/s12984-022-01045-z>.
27. Niu CM, Bao Y, Zhuang C, Li S, Wang T, Cui L, et al. Synergy-based FES for post-stroke rehabilitation of upper-limb motor functions. *IEEE Trans Neural Syst Rehabil Eng*. 2019;27(2):256–64.
28. Fugl-Meyer AR, Jääskö L, Leyman I, Olsson S, Stegling S. A method for evaluation of physical performance. *Scand J Rehabil Med*. 1975;7(1):13–31.
29. Park JH, Shin JH, Lee H, Park CB, Roh J, Park HS. Design and evaluation of a novel experimental setup for upper limb intermuscular coordination studies. *Front Neurobot*. 2019;13(Sept):1–13.
30. Wolf SL, Catlin PA, Ellis M, Archer AL, Morgan B, Piacentino A. Assessing Wolf motor function test as outcome measure for research in patients after stroke. *Stroke*. 2001;32(7):1635–9.
31. Lee DD, Seung HS. Learning the parts of objects by non-negative matrix factorization. *Nature*. 1999;401(6755):788–91.
32. Roland T, Amsuess S, Russold MF, Baumgartner W. Ultra-low-power digital filtering for insulated EMG sensing. *Sensors*. 2019. <https://doi.org/10.3390/s19040959>.
33. Roh J, Cheung VCK, Bizzi E. Modules in the brain stem and spinal cord underlying motor behaviors. *J Neurophysiol*. 2011;106(3):1363–78.
34. Nelles G, Jentzen W, Jueptner M, Müller S, Diener HC. Arm training induced brain plasticity in stroke studied with serial positron emission tomography. *Neuroimage*. 2001;13(6):1146–54.
35. Draganski B, Gaser C, Busch V, Schuierer G, Bogdahn U, May A. Changes in grey matter induced by training. *Nature*. 2004;427(6972):311–2.
36. Boyke J, Driemeyer J, Gaser C, Büchel C, May A. Training-induced brain structure changes in the elderly. *J Neurosci*. 2008;28(28):7031–5.
37. Sampaio-Baptista C, Sanders ZB, Johansen-Berg H. Structural plasticity in adulthood with motor learning and stroke rehabilitation. *Annu Rev Neurosci*. 2018;41:25–40.
38. Hwang S, Min KC, Song CS. Assistive technology on upper extremity function for stroke patients: a systematic review with meta-analysis. *J Hand Therapy*. 2024. <https://doi.org/10.1016/j.jht.2023.12.014>.
39. Chen PM, Kwong PWH, Lai CKY, Ng SSM. Comparison of bilateral and unilateral upper limb training in people with stroke: a systematic review and meta-analysis. *PLoS ONE*. 2019;14(5): e0216357. <https://doi.org/10.1371/journal.pone.0216357>.
40. Kimberley TJ, Pierce D, Prudente CN, Francisco GE, Yozbatiran N, Smith P, et al. Vagus nerve stimulation paired with upper limb rehabilitation after chronic stroke. *Stroke*. 2018;49(11):2789–92.
41. King EC, Pedi E, Stoykov ME, Corcos DM, Urday S. Combining high dose therapy, bilateral motor priming, and vagus nerve stimulation to treat the hemiparetic upper limb in chronic stroke survivors: a perspective on enhancing recovery. *Front Neurol*. 2023;14(June):1–6.

Publisher's Note

Springer Nature remains neutral with regard to jurisdictional claims in published maps and institutional affiliations.